Electronic structure of the gold complexes $Cs_2Au_2X_6$ (X=I, Br, and Cl)

X. J. Liu
Department of Crystalline Materials Science, Nagoya University, Nagoya 464-8603, Japan

K. Matsuda
Department of Applied Physics, Nagoya University, Nagoya 464-8603, Japan

Y. Moritomo*
CIRSE, Nagoya University, Nagoya 464-8601, Japan
and PRESTO, JST, Chiyoda-ku, Tokyo 102, Japan

A. Nakamura
CIRSE, Nagoya University, Nagoya 464-8601, Japan

N. Kojima
Department of Pure & Applied Sciences, University of Tokyo, Tokyo 153, Japan
(Received 2 March 1998; revised manuscript received 14 September 1998)

Electronic structures of halogen bridged mixed-valence (MV) complexes $Cs_2Au_2X_6$ (X=I, Br, and Cl) have been investigated by means of reflectivity measurements. We have observed five polarization-dependent optical transitions in the energy range of 0.6–5.5 eV. The lower-lying three bands below ~3 eV are due to the intermolecular transitions from AuX_2^- to AuX_4^- molecules, while the others are assigned to the intramolecular transitions. The optical gap E_{gap} increases from 1.31 eV for X=I to 2.04 eV for X=Cl, due to enhancement of the nearest-neighboring Coulomb repulsion V and the Jahn-Teller distortion of $AuX_4^-(S)$. We further investigated external pressure effects on the electronic state, and found pressure-induced disappearance of the Raman-active Au-Br stretching modes, which indicates an electronic phase transition from the MV state to a single-valence (SV) state. [S0163-1829(99)11511-X]

I. INTRODUCTION

Mixed-valence metal complexes are attracting current interest due to their characteristic physical properties. Among them, platinum complexes have been extensively studied both experimentally[1–5] and theoretically[6,7] to clarify the nature of the electronic state. In these systems, the strong electron-phonon coupling induces a charge density wave, that is, alternation of the divalence (Pt^{2+}) and tetravalence (Pt^{4+}) sites. In $[Pt(en)_2][Pt(en)_2X_2](ClO_4)_4$ (en =ethylenediamine, X=I, Br, and Cl),[8,9] the optical gap corresponds to the charge-transfer (CT) transition between the neighboring Pt sites, and increases with changing the X^- ions from I^- to Cl^-. Similarly to the chemical substitution, application of hydrostatic pressure affects the electronic state of this system.[10–14]

Gold complex $Cs_2Au_2X_6$ (X=I, Br,and Cl) is another example for the mixed-valence (MV) metal complexes.[15–18] In this system, the Au cations separate into two valence states, i.e., Au^+ and Au^{3+}, and form linear AuX_2^- and square AuX_4^- molecules. These two kinds of molecules align alternately in the tetragonal lattice ($I4/mmm$; $Z=2$),[15–18] and hence this system can be viewed as a molecular system. Kojima and Kitagawa[19] have investigated the electronic structure for $Cs_2Au_2I_6$, and found three optical transitions in the visible region. They have assigned them to the intermolecular CT transitions from AuI_2^- to AuI_4^- molecules. However, a systematic study of the electronic structures with variation of the halogen ions has not been reported. Application of hydrostatic pressure also affects the electronic structure of the MV state via modification of the physical parameters. A pressure-induced tetragonal-to-tetragonal phase transition is reported at 5.5, 9, and 11 GPa for X=I, Br, and Cl, respectively.[20] To clarify the nature of the high-pressure phase, especially on the valence states of Au atoms, we have also performed a high-pressure Raman measurement, which is one of the most sensitive probes for the local symmetry.[21] Our results indicate that the structural transition is of first-order and accompanies changing of the unit cell, i.e., transformation of the electronic state from the MV state to the single-valence (SV) state.

The paper is organized as follows. After describing the experimental procedure in Sec. II, we present the chemical substitution and pressure effects on the electronic state in Sec. III. First, the overall feature of the electronic structure is presented, and the observed transitions are classified into intermolecular and intramolecular types (Sec. III A). We further discuss the systematic change of the optical gap E_{gap} and oscillator strength f with chemical substitution of the X ions in terms of the cluster model (Sec. III B). We performed a high-pressure Raman measurement, and have found a MV-SV transition in $Cs_2Au_2Br_6$ induced by an external pressure of ~7.3 GPa (Sec. III C). We summarize our results in Sec. IV.

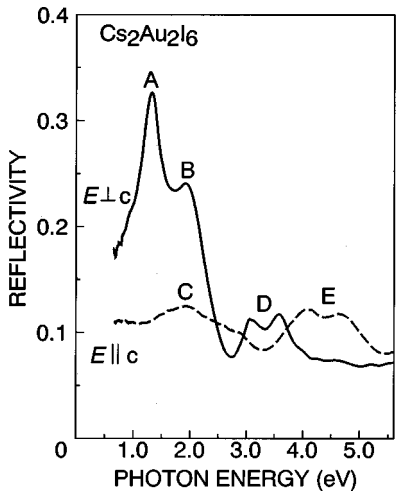

FIG. 1. Polarization dependence of reflectivity spectra for $Cs_2Au_2I_6$ at 300 K. Solid and broken curves represent the spectra with polarization perpendicular ($E\perp c$) and parallel ($E\|c$) to the crystallographic c axis, respectively.

II. EXPERIMENT

The complexes $Cs_2Au_2X_6$ (X=I, Br, and Cl) were synthesized using the same method as reported in Ref. 22. Single crystals were recrystallized from hydrochloric acid solution using an H-type doublet test tube of glass. The obtained crystals were bronze-color square plates, typically 2×2 mm^2 (ab plane) in area and 1 mm (c axis) in thickness. The crystallographic c axis is easily determined using dichroic nature of the crystal.

In reflectivity $R(\omega)$ measurements, a halogen-tungsten lamp (0.6–3.1 eV) and a xenon lamp (2.5–5.5 eV) were used. Light from the lamp was focused with a concave mirror on the entrance slit of a grating monochromator. The monochromatic light was passed through a polarizer and a sharp-cut filter, and was focused on the ac (bc) surface of the sample. Reflected light from the sample was focused on a Si (1.1–5.5 eV) or a Ge (0.6–2.0 eV) photodiode. The absolute reflectivity was obtained by comparison with the reflectance spectrum of an Al mirror.

High-pressure Raman measurements were performed at 300 K using a diamond anvil cell and liquid paraffin as a pressure medium. The applied pressure was monitored using the luminescence peak of a small piece of ruby placed in the gasket hole. At 300 K, pressure inhomogeneity is estimated to be 0.2 GPa above 6 GPa. The sample was excited at 514.5 nm with an argon ion laser in a backward configuration. To avoid the sample damage, the laser power density was kept below 50 W/cm^2. Scattering light was detected with a double monochromator equipped with a photon counting system.

III. RESULTS AND DISCUSSION

A. Overall feature of the electronic structure

Before describing the details of the electronic structures for $Cs_2Au_2X_6$, let us survey the overall feature of the reflectivity $R(\omega)$ spectra. Figure 1 shows the polarization dependence of $R(\omega)$ for $Cs_2Au_2I_6$ at 300 K. Three bands (A, B, and D) are observed for $E\perp c$ and two bands (C and E) for $E\|c$. The lower-lying three bands below ~3 eV (A, B, and C) are assigned to intermolecular transitions from the AuI_2^- to AuI_4^- molecules. The fine structures are due to the crystal-field splitting of the Au5d level as a result of Jahn-Teller-type lattice distortion (site symmetry D_{4h}). In Fig. 2 is shown the splitting of the 5d levels for Au^+ and Au^{3+}. Kojima and Kitagawa[19] have performed a group theoretical analysis on the electronic transitions from Au^+ to Au^{3+} sites, and found three optical transitions related to the 5d level. Judging from polarization dependence, A, B, and C are assigned to the transitions of $5dx^2-y^2\rightarrow5dx^2-y^2$, $5dxy\rightarrow5dx^2-y^2$ and $5dyz(5dzx)\rightarrow5dx^2-y^2$, respectively. In this study, we observed higher-lying weaker bands, i.e., D and E, which can be assigned to intramolecular transitions of the AuI_4^- and AuI_2^- molecules to the Au6s level, respectively. It is noted that the I5p state participates in these two transitions via the strong p-d hybridization with the Au5d state.[23]

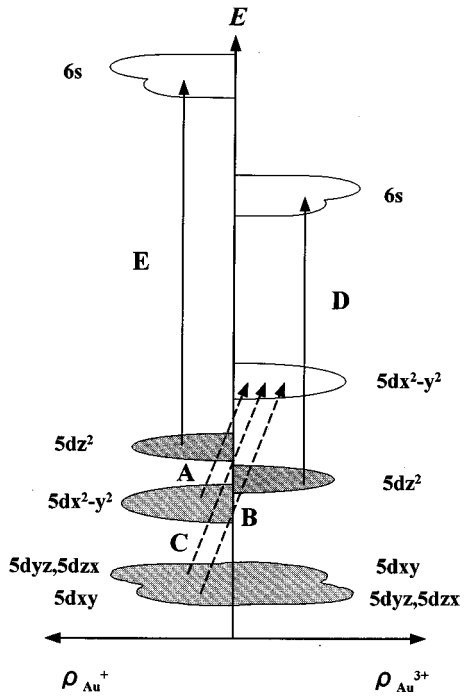

FIG. 2. Schematic electronic structure for $Cs_2Au_2I_6$. Solid and broken arrows are for the intermolecular and the intramolecular transitions, respectively.

Thus obtained electronic structure is schematically shown in Fig. 2. The 5d state of the AuI_2^- molecule is occupied, while the $5dx^2-y^2$ state is empty for the AuI_4^- molecule. The lower-lying three optical transitions (broken arrows) are characterized by the charge-transfer (CT) type from AuI_2^- to AuI_4^- molecules, while the higher-lying two transitions (solid arrows) are of the intramolecular type.

B. Charge-transfer transitions in the mixed-valence state

Chemical substitution of halogen ions significantly affects the electronic structure. Figure 3 shows $R(\omega)$ for $Cs_2Au_2X_6$ (X=Cl, Br,and I) for $E\perp c$ at 300 K. Substitution of Br^- (or Cl^-) ions for I^- ions does not change the overall feature of the spectra, but induces a blue-shift of the peak energies. In order to estimate the optical parameters pre-

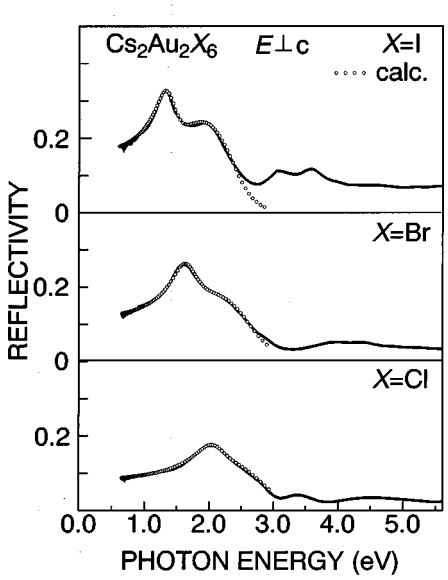

FIG. 3. Reflectivity spectra ($E\perp c$) for $Cs_2Au_2X_6$ (X=I, Br, and Cl) at 300 K. Open circles are the best-fitted results with a two-Lorentz oscillator model.

cisely, the spectra were analyzed with a two-Lorentz oscillator model. According to the model, the dielectric function ϵ is expressed as

$$\epsilon=\epsilon_1-i\epsilon_2=\epsilon_\infty+\frac{4\pi\alpha_A\omega_A^2}{\omega_A^2-\omega^2+i\Gamma_A\omega}$$

$$+\frac{4\pi\alpha_B\omega_B^2}{\omega_B^2-\omega^2+i\Gamma_B\omega}, \tag{1}$$

where α_i, ω_i, and Γ_i (i=A and B) are the polarizability, resonance energy, and damping constant, respectively. The refractive index n, extinction coefficient κ, and reflectivity R can be calculated as

$$n^2(\omega)=\frac{\sqrt{\epsilon_1^2+\epsilon_2^2}+\epsilon_1}{2}, \tag{2}$$

$$\kappa^2(\omega)=\frac{\sqrt{\epsilon_1^2+\epsilon_2^2}-\epsilon_1}{2}, \tag{3}$$

and

$$R=\frac{(n(\omega)-1)^2+\kappa^2(\omega)}{(n(\omega)+1)^2+\kappa^2(\omega)}. \tag{4}$$

The oscillator strength f_i is expressed as

$$f_i=\frac{\alpha_i\omega_i^2 m_0}{N_0 e^2}, \tag{5}$$

where N_0 is the reciprocal of the unit cell volume, m_0 and e are the mass and charge of an electron, respectively. Open circles in Fig. 3 show the best-fitted spectra. The obtained parameters are listed in Table I. The energy difference between A and B bands, which is a crude measure of the crystal-field splitting, is nearly the same ($\sim$0.5 eV) for all the complexes. The f value per Au pair decreases from $f_A=0.83$ ($f_B=1.69$) for X=I to $f_A=0.58$ ($f_B=1.01$) for X=Cl, due to the decreasing hybridization between the Au5d and Xnp orbitals. Similar chemical substitution effects on the oscillator strength have been reported in the halogen-bridged MV platinum complexes, $[Pt(en)_2][PtX_2(en)_2](ClO_4)_4$ (en=ethylenedyamine, X=I, Br, and Cl.)[8]

TABLE I. Resonance frequency ω_i, oscillator strength f_i per Au pair, and damping constant Γ_i (i=A and B) for $Cs_2Au_2X_6$ (X=I, Br, and Cl).

X		ω_i (eV)	f_i	Γ_i (eV)
I	$i=A$	1.31	0.83	0.32
	$i=B$	1.82	1.69	0.92
Br	$i=A$	1.60	0.71	0.41
	$i=B$	2.10	1.32	1.17
Cl	$i=A$	2.04	0.58	0.54
	$i=B$	2.50	1.01	1.24

Now let us discuss the chemical substitution effect on the optical gap in terms of the Jahn-Teller splitting (S), on-site (U) and nearest-neighboring (V) Coulomb repulsions. Here, we will consider an isolated cluster of seven molecules, namely a square $AuCl_4^-$ molecule surrounded by six linear $AuCl_2^-$ molecules [see Fig. 4(a)]. In the ground state, elec-

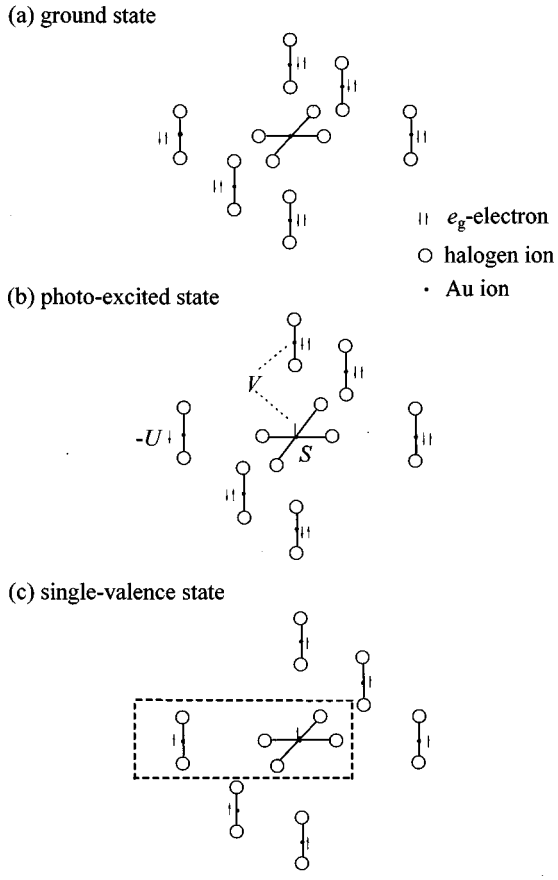

FIG. 4. Schematic picture for $(AuX_4^-)(AuX_2^-)_6$ cluster: (a) ground state, (b) photoexcited state, and (c) single-valence state.

TABLE II. Distance L between the neighboring Au sites and halogen displacement δ from the central position for $Cs_2Au_2X_6$ (X=I, Br, and Cl).

X		L (Å)	δ (Å)	$2\delta/L$	Ref.
I	c	6.046	0.437	0.145	16
	ab	5.858	0.283	0.097	16
Br	c	5.654	0.424	0.150	17
	ab	5.487	0.305	0.111	17
Cl	c	5.440	0.439	0.161	18
	ab	5.300	0.355	0.134	18

tron pairs are localized at the alternating Au sites due to gain of the Jahn-Teller-type lattice distortion. In this model, the excitation energy $E_{\rm gap}$ is expressed as $S-U+11V$, where the last term comes from the nearest-neighboring Coulomb repulsion V [see Fig. 4(b)]. Table II lists the typical lattice parameters for $Cs_2Au_2X_6$,[16–18] i.e., intersite distance L and halogen displacement δ from the central position between the neighboring Au sites. With decreasing atomic number of the halogen ions, i.e., in the order of I^-, Br^-, and Cl^-, the L value decreases and the value of δ/L increases. Resultant enhancement of V and S is expected to increase $E_{\rm gap}$, as observed.

Here, let us consider the highly photoexcited state. If many electrons were photoexcited onto the Au^{3+} sites, the smaller number of electrons at the Au^+ sites would reduce the excitation energy. In an extreme case where half of the electrons are photoexcited, the energy difference from the MV ground state is $\Delta E=S-U+6V$ per one electron pair [see Fig. 4(c)]. Note that the ΔE value is much smaller than the optical gap, implying a possible photoinduced phase transition from the MV state to a SV state via the highly photoexcited state. Such a SV state is achieved by application of an external hydrostatic pressure (*vide infra*).

C. Single-valence state induced by an external pressure

Before describing details of the pressure effects on the Raman spectra, let us consider the Raman activity of the Au-X stretching modes. $Cs_2Au_2X_6$ crystal consists of linear AuX_2^- (site symmetry D_{4h}) and square AuX_4^- (D_{4h}) molecules. The other vibrational modes, such as bending-type modes and vibrational modes of the heavy Cs^+ ions, would occur in the lower-frequency region below $\sim$100 cm^{-1}. The group theoretical analysis tells us that enumeration of the Au-X stretching modes for the square AuX_4^- molecule is $A_{1g}+B_{1g}+E_u$, and that for the linear AuX_2^- molecule is $A_{1g}+A_{2u}$. Among them, three modes, i.e., $2A_{1g}+B_{1g}$, are Raman active. Figure 5 shows the Raman spectra for $Cs_2Au_2X_6$ (X=Cl and Br) at ambient pressure. Two A_{1g} modes are observed in the $c(a+b,a+b)\bar{c}$ configuration, while one B_{1g} mode is observed in the $c(a+b,a-b)\bar{c}$ configuration. Judging from the longer Au-Cl bond (2.295 Å) in the $AuCl_4^-$ molecule as compared with the bond (2.281 Å) in the $AuCl_2^-$ molecule,[18] the lower-lying two modes, i.e., B_{1g} (297 cm^{-1}) and A_{1g} (2.99 cm^{-1}) modes, are ascribed to the square $AuCl_4^-$ molecule. The higher-lying A_{1g} (324 cm^{-1}) mode is due to the linear $AuCl_2^-$ molecule.

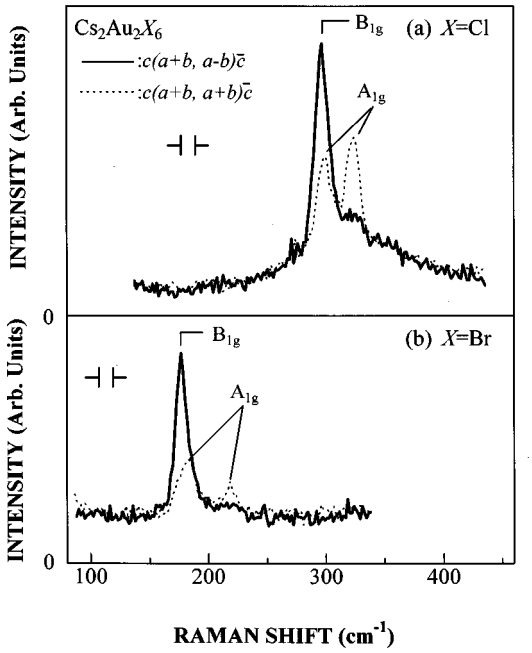

FIG. 5. Raman scattering spectra for $Cs_2Au_2X_6$ at 300 K: (a) X=Cl and (b) X=Br. Solid and broken curves are the spectra with configurations of $c(a+b,a-b)\bar{c}$ and $c(a+b,a+b)\bar{c}$, respectively.

Frequencies of the stretching modes are significantly reduced in $Cs_2Au_2Br_6$ [see Fig. 5(b)], as compared with that in $Cs_2Au_2Cl_6$. The ratios $\omega_{\rm Au\text{-}Br}/\omega_{\rm Au\text{-}Cl}$ of the frequencies are 0.61 and 0.67 for the lower-lying and higher-lying A_{1g} modes and 0.60 for the B_{1g} mode, which are all close to the ideal value [$0.67=(m_{\rm Cl}/m_{\rm Br})^{1/2}$]. We also found a significant resonant effect in the Raman spectra of $Cs_2Au_2Br_6$, reflecting strong electron-lattice interaction.

Figure 6 shows pressure dependent Raman spectra for $Cs_2Au_2Br_6$. The high-pressure Raman measurements were performed in an unpolarized configuration.[24] Intensity of the strongest B_{1g} mode is plotted in Fig. 7(a) against pressure. Open and closed circles show the data obtained in the pressure-applying and pressure-reducing runs, respectively. Although the intensity is almost constant below $\sim$4 GPa, it suddenly decreases around 6 GPa and disappears above $\sim$7.3 GPa (open circles). This indicates that the Br^- ions shift to the central position between the neighboring Au sites under pressure above $\sim$7.3 GPa. In this structure, enumeration of the Au-X stretching modes would change into E_u+A_{2u}, and the Raman-active modes should disappear. In other words, the two Au sites become equivalent and a single-valence (SV) state is achieved. The steep drop of the intensity as well as the prominent pressure hysteresis (hatched region) indicates a first-order nature of the MV-SV transition.

Finally, let us discuss pressure-induced shifts of the Raman modes. In Fig. 7(b) are shown the pressure-shifts of the B_{1g} mode and A_{1g} mode. The former and the latter are due to the Au-Br stretching vibrations in the $AuBr_4^-$ and $AuBr_2^-$ molecules, respectively. Open and closed circles stand for the pressure-applying and pressure-reducing runs, respectively. As indicated by the eye-guided curve in Fig. 7(b), the B_{1g} mode shows a significant softening (-2.1 cm^{-1}/GPa), making a sharp contrast with a slight hardening of the A_{1g} mode. A similar softening of B_{1g} (-5.8 cm^{-1}/GPa) is also

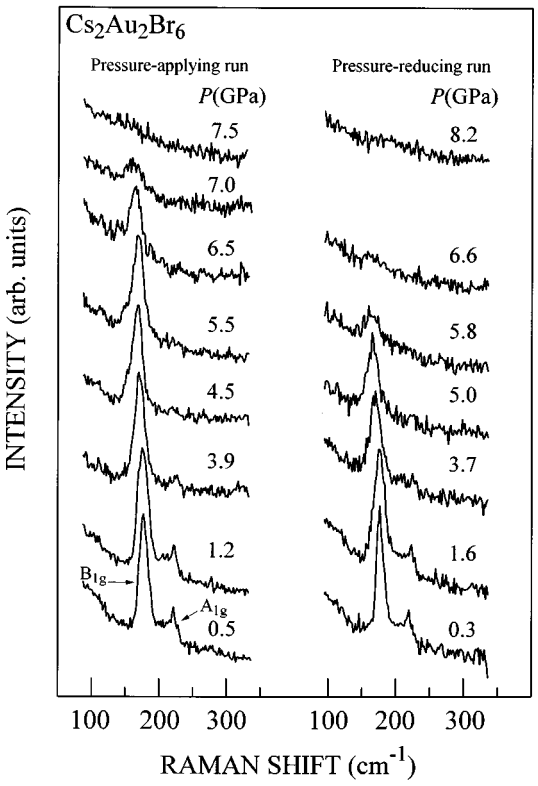

FIG. 6. Pressure dependence of the Raman spectra for $Cs_2Au_2Br_6$ at 300 K with the unpolarized configuration. The left and right spectra are for the pressure-applying and pressure-reducing runs, respectively.

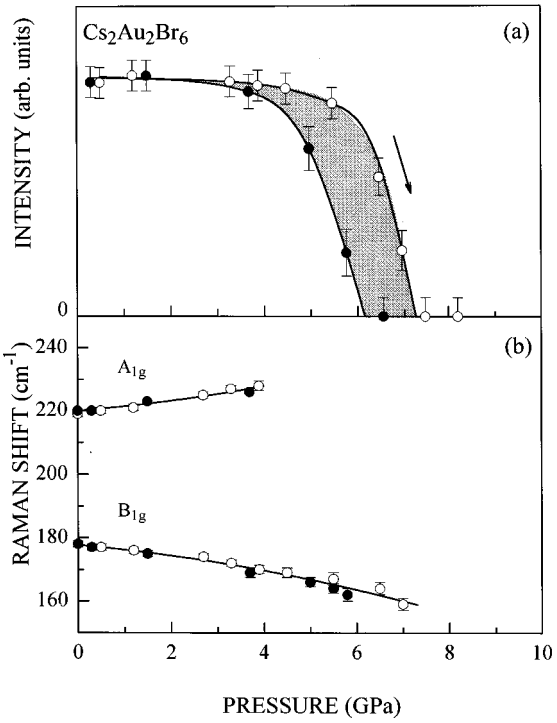

FIG. 7. Pressure variation of (a) intensity and (b) frequencies of the Au-Br stretching modes for $Cs_2Au_2Br_6$. Open and closed circles show the data obtained in the pressure-applying and pressure-reducing runs, respectively. Curves are the guide to the eyes. Hatching represents a pressure hysteresis.

observed for $Cs_2Au_2Cl_6$ (not shown).[25] The softening suggests weakening of the Au-Br bonds with the Jahn-Teller distorted $AuBr_4^-$ molecules.

IV. SUMMARY

We have systematically investigated the variation of the electronic structures of $Cs_2Au_2X_6$ with changing the halogen ions from I to Cl. The observed optical transitions are classified according to intermolecular and intramolecular types. Variation of optical gap with chemical substitution is ascribed to the enhanced V and S values. We further observed a pressure-induced transition from the MV state to the SV state.

ACKNOWLEDGMENTS

This work was supported by a Grant-In-Aid for Scientific Research from the Ministry of Education, Science, Sport and Culture, Japan and from Precursory Research for Embryonic Science and Technology (PRESTO), Japan Science and Technology Corporation (JST), Japan.

*Author to whom correspondence should be addressed.

[1] M. Kurmoo and R. J. H. Clark, Inorg. Chem. **24**, 4420 (1985).
[2] Y. Wada, T. Mitani, K. Toriumi, and M. Yamashita, J. Phys. Soc. Jpn. **58**, 3013 (1989).
[3] N. Kuroda, M. Sakai, M. Suezawa, Y. Nishina, and K. Sumino, J. Phys. Soc. Jpn. **59**, 3049 (1990).
[4] L. Degiorgi, P. Wachter, M. Haruki, and S. Kurita, Phys. Rev. B **40**, 3285 (1989); **41**, 573 (1990).
[5] R. J. Donohoe, R. B. Dyer, and B. I. Swanson, Solid State Commun. **73**, 521 (1990).
[6] K. Nasu, J. Phys. Soc. Jpn. **52**, 3865 (1983); **53**, 302 (1984); **53**, 427 (1984).
[7] J. Tinka Gammel, A. Saxena, I. Batistic, and A. R. Bishop, Phys. Rev. B **45**, 6408 (1992); S. M. Weber-Millbrodt, J. Tinka Gammel, A. R. Bishop, and E. Y. Loh, Jr., *ibid.* **45**, 6435 (1992).
[8] Y. Wada, T. Mitani, M. Yamashita, and T. Koda, J. Phys. Soc. Jpn. **54**, 3143 (1985).
[9] B. Scott, S. P. Love, G. S. Kanner, S. R. Johnson, M. P. Wilkerson, M. Berkey, B.I. Swanson, A. Saxena, X. Z. Huang, and A. R. Bishop, J. Mol. Struct. **356**, 207 (1995).
[10] H. Tanino, N. Koshizuka, K. Kobayashi, M. Yamashita, and K. Hoh, J. Phys. Soc. Jpn. **54**, 483 (1985).
[11] M. Saki, N. Kuroda, and Y. Nishina, Phys. Rev. B **40**, 3066 (1989).
[12] N. Kuroda, M. Sakai, and Y. Nishina, Phys. Rev. Lett. **68**, 3056 (1992).
[13] A. Girlando and A. Painelli, Synth. Met. **55–57**, 3407 (1993).
[14] G. S. Kanner, J. Tinka Gammel, S. P. Love, S. R. Johnson, B. Scott, and B. I. Swanson, Phys. Rev. B **50**, 18 682 (1994).
[15] N. Elliott and L. Pauling, J. Am. Chem. Soc. **60**, 1846 (1938).
[16] N. Matsushita, H. Kitagawa, and N. Kojima, Acta Crystallogr., Sect. C: Cryst. Struct. Commun. **53**, 663 (1997).
[17] N. Kojima, N. Matushita, A. Tanaka, M. Seto, and Yu. Maeda, J.

Chem. Soc. Dalton Trans. (to be published).
[18] J. C. M. Tindemans-v. Eijndhoven and G. C. Verschoor, Mater. Res. Bull. **9**, 1667 (1974).
[19] N. Kojima and H. Kitagawa, J. Chem. Soc. Dalton Trans. **1994**, 327.
[20] N. Kojima, M. Hasegawa, H. Kitagawa, and O. Shimomura, J. Am. Chem. Soc. **116**, 11 368 (1994).
[21] For example, see Y. Moritomo, Y. Tokura, N. Nagosa, T. Suzuki, and K. Kumagai, Phys. Rev. Lett. **71**, 2833 (1993).
[22] H. Kitagawa, N. Kojima, N. Matsushita, T. Ban, and I. Tsujikawa, J. Chem. Soc. Dalton Trans. **1991**, 3115; H. Kitagawa, N. Kojima, and T. Nakajima, *ibid.* **1991**, 3121.
[23] M. Shirai, Synth. Met. **55–57**, 3389 (1993).
[24] The strongest B_{1g} mode inevitably overlaps on the lower-lying A_{1g} mode. Note that the intensity of the B_{1g} [see Fig. 7(a)] includes that of the overlapped weaker A_{1g} mode.
[25] The critical pressure for the MV-SV transition seems to be greater than $\sim$10 GPa, which is the maximum pressure of our high-pressure apparatus.